JOURNAL OF APPLIED ELECTROCHEMISTRY 19 (1989) 697–702

New electrodes for oxygen evolution in acidic solution*

P. A. DYKSTRA, G. H. KELSALL

Department of Mineral Resources Engineering, Royal School of Mines, Imperial College, London SW7 2BP, UK

X. LIU, A. C. C. TSEUNG

Department of Chemistry & Biological Chemistry, University of Essex, Wivenhoe Park, Colchester CO4 3SQ, UK

Received 1 November 1988

Conventional electrowinning of metals such as zinc and copper from 1–1.5 kmol m^{-3} H_2SO_4 electrolytes involves anodic oxygen evolution at Pb alloy/PbO_2 anodes operating at 200–800 A m^{-2}. The oxygen overpotential, estimated to be about 0.6 V, constitutes a significant proportion of the cell voltage (typically 2.5 V for Cu and 3.3 V for Zn). The objective of this work was to lower the anode overpotential and so decrease the process specific energy requirements, by devising new anode materials based on: (1) PTFE-bonded PbO_2 catalysts, supported on Pb–Ag alloys; (2) modification of the pore structure of porous electrodes to maximize the utilization of the available surface without the use of PTFE bonding. Both methods are shown to produce significant benefits in lowering oxygen overpotentials, though the latter technique has been tested only in alkaline electrolytes, as yet. However, with the former approach, substrate oxidation through the porous catalyst layer has been found to cause catalyst shedding after > 60 h at 1 kA m^{-2}, though careful pre-oxidation of the anode substrate appears to extend the anode life.

(∀)

1. Introduction

Oxygen evolution on the Pb/PbO_2 anodes presently used, for example in metal (Zn, Cu, Co etc.) electrowinning from acidic sulphate electrolytes, requires high anode potentials due to the poor catalytic properties of PbO_2 for the reaction:

$$2H_2O = O_2 + 4H^+ + 4e^- \quad (1)$$

The anode overpotential has been estimated as about 0.6 V [1] at typical electrowinning current densities (200–800 A m^{-2}); this constitutes a major component of the specific energy requirements for any such electrolytic process.

For example, in roast–leach–electrowin processes used in the production of about 80% of the world's 6×10^6 tonne Zn $year^{-1}$ [2], the total oxygen overpotential constitutes about 20% of the 3.3 V cell voltage, or 600 kWh $tonne^{-1}$, a saving of 0.25 V in anode potential/cell voltage would decrease the specific energy requirement by 250 kWh (tonne Zn)$^{-1}$.

Two methods of decreasing the anode overpotential are reported here: (a) increasing the active area of the electrocatalyst to lower the real current density, i.e. by changing the structure of the currently used planar Pb/PbO_2 anode to PTFE-bonded high specific surface area lead dioxide anodes; (b) modifying the pore structure of the oxygen-evolving anode to achieve more efficient utilization of the available area without the use of PTFE bonding.

Electron microscopy has shown that PTFE-bonded electrocatalyst structures comprise two porous, continuous phases intimately intermingled [3]. The porous electrocatalyst phase is hydrophilic and is filled with electrolyte when in use; the porous hydrophobic PTFE phase remains dry and allows rapid diffusion of gas out of the electrocatalyst aggregates. However, there are potentially two disadvantages of using PTFE particles as the catalyst binder: (a) relatively low mechanical strength of the catalyst layer; (b) increase resistance, exacerbated by the hydrophobic PTFE surface causing larger gas bubbles to adhere by surface tension forces, so increasing electrolyte phase potential losses.

2. Experimental details

2.1. *Preparation of PTFE-bonded electrodes*

PbO_2 electrocatalyst was added in the mass ratio of 10 : 3 to a polytetrafluoroethylene (PTFE) dispersion and the resulting catalyst slurry painted onto a Pb foil current collector, which had been lightly roughened using 400 grade SiC paper. The catalyst was dried in a stream of hot air and successive layers applied to increase loading. The electrode was then placed in an oven and sintered at 300° C for 1 h.

A dynamic hydrogen electrode (DHE) reference electrode was used with a 4 cm^2 platinum foil counter-electrode in 1.5 or 2 kmol H_2SO_4 m^{-3}.

* Paper presented at the 2nd International Symposium on Electrolytic Bubbles organized jointly by the Electrochemical Technology Group of the Society of Chemical Industry and the Electrochemistry Group of the Royal Society of Chemistry and held at Imperial College, London, 31st May and 1st June 1988.

0021-891X/89 $03.00 + .12 © 1989 Chapman and Hall Ltd.

2.2. *Conductivity measurements*

A four-point probe was used to measure the resistivites of lead dioxide/PTFE mixtures prepared on glass and lead substrates. Current was supplied via a Thompson 'Ministat' operating as a galvanostat. All current and voltage measurements were made using a Keithley 150B microvoltmeter/ammeter. The thickness of the prepared samples were measured using a travelling microscope. As well as the lead oxide/PTFE mixture, an indium-doped SnO_2-coated glass slide was electroplated with β-PbO_2 by passing $5\,mA\,cm^{-2}$ through a saturated solution of lead(II) acetate; the PbO_2 thickness was calculated from the charge passed, assuming 100% current efficiency. Also, a glass slide was coated with β-PbO_2 by hydrolysis of lead(IV) acetate.

2.3. *Cyclic voltammetry and resistometry*

A Solartron 1286 potentiostat and 1250 frequency response analyser (FRA) controlled by an IBM AT microcomputer were used for cyclic voltammetry with simultaneous resistance and capacitance measurements on lead-substrated anodes. Cyclic voltammetry was performed with a potential sweep rate of $10\,mV\,s^{-1}$ whilst a 10 kHz a.c. potential perturbation of 3.5 mV peak-to-peak was applied via the FRA. The high frequency measurements enabled the total uncompensated ohmic resistance, R_u, to be determined as the real component of the interfacial impedance. This included resistances due to contact, bulk electrode, surface film and electrolyte between electrode surface and Luggin probe tip. Hence, the time/potential varying part of R_u can be attributed to changes in the structure of the interphase and to bubbles on the electrode or between it and the Luggin probe tip in the electrolyte.

3. Results and discussion

3.1. *Pb/PbO_2/PTFE-bonded electrodes*

The potential/current performance of a Pb/$110\,g\,m^{-2}$ PTFE-bonded β-PbO_2 electrode and that for a Pb/PbO_2 electrode is shown in Fig. 1, which indicates that the PTFE-bonded anode achieved approximately 100 mV saving in potential at $500\,A\,m^{-2}$. Tafel slopes for both anodes were approximately 120 mV decade^{-1}, in agreement with previously reported values for Pb/PbO_2 anodes [4]. However, the lifetime of PTFE-bonded electrodes was found to be limited by oxidation of the lead substrate, causing detachment of catalyst layers after say >60 h operation, though careful pre-oxidation of the anode substrate is being found to extend the life. With less oxidizable substrates such as Ti, lifetimes in excess of 20 days have been achieved with potential savings of >0.2 V.

The improvement in performance of the PTFE-bonded electrode compared with a planar lead–silver alloy anode is not as high as expected from the scale-up in surface area of the lead dioxide, as calculated from the PbO_2 particle size used in the composite anode. At least three factors could be responsible: (a) aggregate size; (b) resistivity of the PTFE-catalyst mix; (c) blinding of exterior catalyst surfaces by gas bubbles, which adhere preferentially to the hydrophobic PTFE, causing larger diameter bubbles than at nominally hydrophilic surfaces due to surface tension forces.

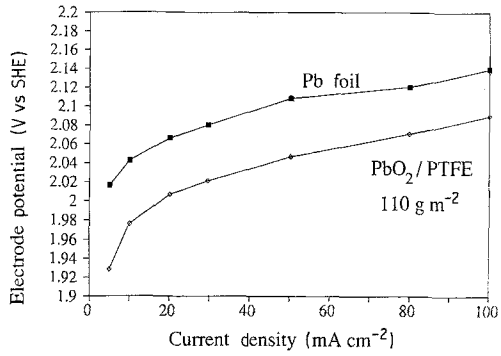

Fig. 1. Comparison of the anodic oxygen evolution performance of planar oxidized Pb and Pb/$110\,g\,m^{-2}$ PTFE-bonded β-PbO_2 in $2\,kmol\,m^{-3}$ H_2SO_4 at 333 K.

Scanning electron microscopic investigation showed that the average aggregate size of the β-PbO_2 powder was about $1.5\,\mu m$; this corresponds to a scale-up in catalyst area of about 43 times the geometric area at $100\,g\,m^{-2}$ PbO_2 loading. For *iR*-corrected Tafel slopes of 120 mV decade^{-1}, this would produce a potential saving of about 190 mV if all aggregate surfaces were uniformly active.

3.1.1. PbO_2/PTFE resistivity measurements. The resistivity of electrodeposited β-PbO_2, at 10^{-6} ohm m [5], is comparable to that of lead (2.06×10^{-7} ohm m). Resistivities were calculated from four-point probe measurements using a theorem developed by van der Pauw [6] for the specific resistivity of a flat sample of arbitrary shape, without the requirement of knowing the current density distribution.

The results for lead dioxide/PTFE layers coated onto glass slides are reported in Table 1. The resistivities of lead dioxide/PTFE layers at 10^{-3}–10^{-5} ohm m were approximately 2–3 orders of magnitude greater than that of an electrodeposited film of β-PbO_2 (10^{-7} ohm m). As would be expected, the resistivity

Table 1. Resistivities by PbO_2/PTFE mixtures on glass substrates

Sample	*Loading ($g\,m^{-2}$)*	*Resistivity (ohm m)*
Electrodeposited β-PbO_2		2×10^{-7}
Hydrolysis deposit β-PbO_2		4.5×10^{-4}
β-PbO_2 from Pb_3O_4 + HNO_3	103	4.9×10^{-3}
β-PbO_2 as above	221	3.8×10^{-5}
α-PbO_2	112	1.64×10^{-3}
α-PbO_2	176	7.8×10^{-4}

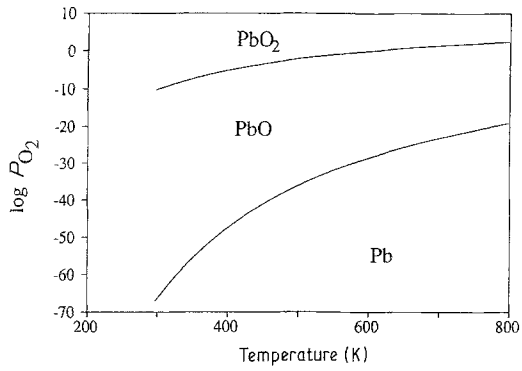

Fig. 2. Equilibrium oxygen partial pressures in the Pb–O system as a function of temperature.

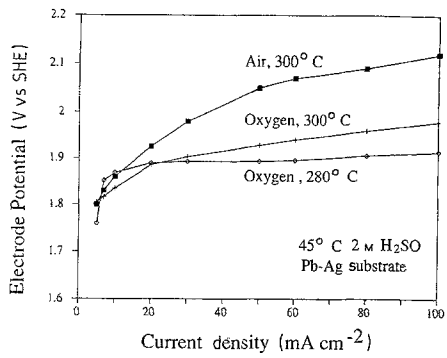

Fig. 4. Effect of catalyst layer sintering conditions on the performance of Pb–0.5% Ag/PbO_2/PTFE-bonded anodes for oxygen evolution in 2 kmol m^{-3} H_2SO_4 at 318 K.

increased with the introduction of a non-conductive phase such as PTFE into the conducting PbO_2 phase. Also, it can be seen that the higher the loading of PbO_2, the lower the calculated resistivity, i.e. for 221 g m^{-2} β-PbO_2, $\varrho = 3.8 \times 10^{-5}$ ohm m whereas for 103 g m^{-2} β-PbO_2, $\varrho = 4.9 \times 10^{-3}$ ohm m.

The effect on the conductivity of a continuous conducting phase by the inclusion of a dielectric phase (such as PTFE) present at some volumetric void fraction ε, is a classical problem which has been reviewed [7]. Several correlations are available relating the effective resistivity (ϱ_{eff}) to the bulk continuous phase conductivity and the void fraction (ε) in that conducting phase due to the dispersed dielectric phases. The most commonly used of these correlations is due to Bruggeman [8]:

$$\varrho_{eff} = \varrho(1 - \varepsilon)^{-1.5} \tag{2}$$

In the case of PbO_2/PTFE mixtures the volumetric void fraction ε was calculated as approximately 0.6. Equation 2 then predicts a fourfold increase in resistivity from that of continuous phase lead dioxide. Table 1 shows clearly a 10–100 times increase in resistivity from that of bulk lead dioxide, indicating some other factor was predominating.

3.1.2. Effect of sintering conditions. Thermodynamic data [9] were used to calculate the partial pressure of oxygen over the two stoichiometric lead oxides as a function of temperature:

$$2PbO + O_2 = 2PbO_2 \tag{3}$$

$$2Pb + O_2 = 2PbO \tag{4}$$

Assuming the oxides to be pure solids of unit activity, i.e. neglecting the non-stoichiometric phases for which reliable Gibbs energies of formation are not available, then:

$$\log P_{O_2} = \frac{\Delta G^0}{2.303RT} \tag{5}$$

As ΔH and ΔS are functions of temperature, ΔG_T^0 does not vary linearly with temperature. The temperature dependence of ΔH may be derived from an empirical power series for molar heat capacity at constant temperature:

$$\Delta C_p = \Delta a + \Delta bT + \Delta cT^2 = \left(\frac{d(\Delta H)}{dT}\right)_p \tag{6}$$

Hence, by integrating Equation 6:

$$\Delta H_T = \Delta H_0 + \Delta aT + \frac{\Delta bT^2}{2} + \frac{\Delta cT^3}{3} \tag{7}$$

and as:

$$\frac{d(\Delta G/T)}{dT} = -\frac{\Delta H}{T^2} \tag{8}$$

by integration:

$$\Delta G_T^0 = \Delta H_0 - \Delta aT \ln T - \frac{\Delta bT^2}{2} - \frac{\Delta cT^3}{6} + IT \tag{9}$$

where I is an integration constant, determined from ΔG_{298} and ΔH_0. The coefficients in Equations 6, 7 and 9 were as follows [10].

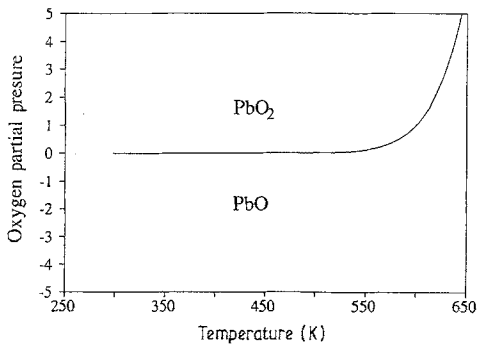

Fig. 3. Equilibrium oxygen partial pressures for the PbO_2/PbO reaction as a function of temperature.

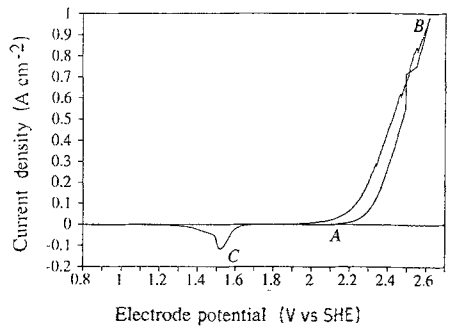

Fig. 5. Cyclic voltammogram of Pb/1.5 kmol m^{-3} H_2SO_4, 10 mV s^{-1}.

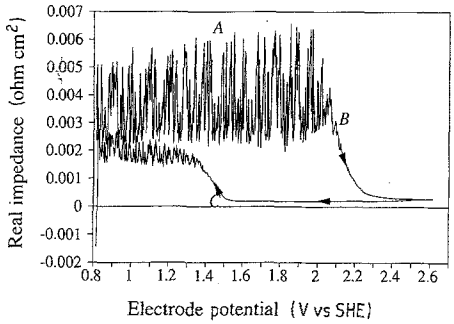

Fig. 6. Cyclic resistogram of Pb/1.5 kmol m^{-3} H_2SO_4, 10 mV s^{-1}.

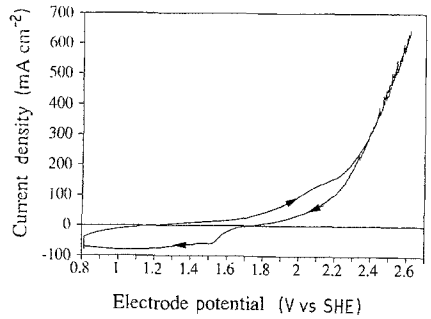

Fig. 8. Cyclic voltammogram of Pb/300 g m^{-2} PTFE-bonded β-PbO_2/1.5 kmol m^{-3} H_2SO_4, 10 mV s^{-1}.

Coefficient	Reaction (3)	Reaction (4)
Δa/kJ mol^{-1} K^{-1}	−16.99	6.93
Δb/kJ mol^{-1} K^{-2}	0.03074	13.16 × 10^{-3}
Δc/kJ mol^{-1} K^{-3}	1.94 × 10^{-5}	1.94 × 10^{-5}

The predicted equilibrium oxygen partial pressures as functions of temperature, for Reactions 3 and 4, are given in Fig. 2, the lines defining the equilibrium conditions at which pairs of the solids coexist. Figure 3 shows an enlargement of the data from Fig. 2 for Reaction 3. At the typical sintering temperature of 598 K for the PbO_2/PTFE electrocatalysts, the equilibrium oxygen pressure is 1.01 atm, so that in air (P_{O_2} = 0.21) conditions are slightly reducing; hence PbO_2 may decompose to PbO, evolving oxygen by the reverse reaction of Equation 3. The associated decrease in molar volume would expose the substrate, which, according to Fig. 2, would oxidize thermally by Reaction 4, leading to decreased catalyst adhesion to the lead. These thermodynamic predictions are congruous with the observation of some thermal reduction of PbO_2 to yellow PbO (c) occurring at 598 K.

Thermogravimetric analysis (TGA) and differential thermal analysis (DTA) were used to study the thermal stability/decomposition of PbO_2 as a function of temperature and oxygen pressure. At heating rates of 40° C min^{-1} the percentage weight loss in lead dioxide, after the loss of sorbed water, was 0.92, 1.39 and 0 mass% for static air, 43.5 cm^3 min^{-1} N_2 and 43.5 cm^3 min^{-1} O_2, respectively. These figures agree with the thermodynamic predictions of lead dioxide reduction during sintering in air, the extent of reduction being increased in a nitrogen atmosphere and essentially suppressed in pure oxygen. The presence of lower oxides in the PbO_2/PTFE catalyst explains why the measured resistivities were so much higher than the values predicted solely from their phase ratios; hence the need to sinter the catalyst in pure oxygen using the lowest practical sintering temperature.

Although anodic oxygen evolution on the partially reduced catalyst may re-inject the oxygen deficiency, any lead substrate area exposed to the electrolyte will also oxidize, the resulting molar volume increase adversely affecting catalyst adhesion, leading to shedding and eventual anode failure. Comparison of the oxygen evolution performance (Fig. 4) of anodes sintered in air and in oxygen showed that the former environment produced inferior electrodes and that any injection of the oxygen deficiency by electrochemical means did not improve their performance with time in service.

The four-point probe method of measuring the electrical conductivity of the PbO_2/PTFE-bonded catalyst layers is necessarily parallel to the support (glass), so that structural discontinuities in the layer will greatly decrease its conductivity, whereas in service, it is the conductivity perpendicular to the (Pb) substrate which is important; for thin catalyst layers, it is most likely that the conductivity is anisotropic. Also, conductivities measured *ex situ* may differ substantially from the resistivities of the catalyst layer when polarized at high anodic potentials. Hence, impedance spectroscopy was used to measure electrode resistance (and capacitance) as a function of anode potential and service history.

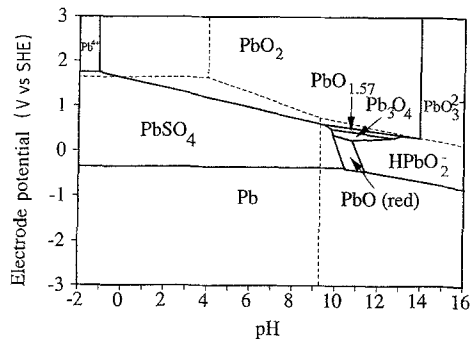

Fig. 7. Potential–pH diagram for the Pb–SO_4^{2-}–H_2O system at 298.15 K and dissolved activities of 10^{-4} and 2 for lead and sulphate, respectively. Data from [10].

3.1.3. Cyclic voltammetry and resistometry. The cyclic voltammogram and cyclic resistogram of Pb/2 kmol m^{-3} H_2SO_4 are shown in Figs 5 and 6. In the voltammogram, according to the potential–pH diagram in Fig. 7, region A corresponds to the nucleation and growth of β-PbO_2 from $PbSO_4$:

$$PbSO_4 + 2H_2O \longrightarrow PbO_2(\beta) + HSO_4^- + 2e^-$$

$$E_{10}(V) = 1.6230 - 0.0887pH + 0.0296 \log (HSO_4^-) \quad (10)$$

On reversing the scan, region B corresponds to oxygen evolution on β-PbO_2, and region C to the reduction of

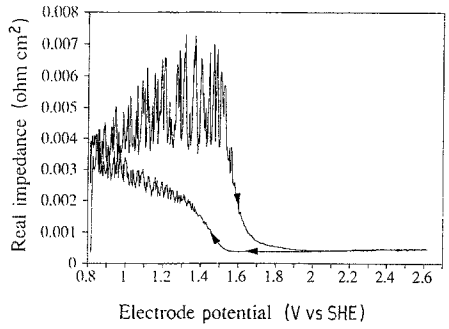

Fig. 9. Cyclic resistogram of Pb/300 g m^{-2} PTFE-bonded β-PbO_2/1.5 kmol m^{-3} H_2SO_4, 10 mV s^{-1}.

β-PbO_2 to $PbSO_4$. In the corresponding resistogram, region A shows noise which was probably due to molar volume changes in the $PbSO_4$ layer as oxidation to β-PbO_2 occurs. The molar volume of β-PbO_2 (25 cm^3 mol^{-1}) is much less than that of $PbSO_4$ (48 cm^3 mol^{-1}) and so pores are created in the outer $PbSO_4$ layer. β-PbO_2 is a quasi-metallic conductor and so the electrode resistance decreased as this was formed in region B. This rise of resistance in region C was probably due to the formation of $PbSO_4$ as β-PbO_2 is reduced. These results are in broad agreement with a previous measurement of the cyclic resistance of a lead electrode in sulphuric acid electrolytes [11].

The cyclic voltammogram (Fig. 8) and resistogram (Fig. 9) for an anode comprising a lead substrate with 260 g m^{-2} PbO_2/PTFE coating, were far less well defined in potential terms, compared to those observed with lead alone; this was due to the structure of the former anode and the associated distribution of potential within the porous catalyst layer, particularly once reduced to less conducting phases. In the resistogram, the collapse of resistance on the positive-going potential sweep occurred at 1.6 V vs SHE compared with 2.1 V vs SHE for lead, and the high potential resistance value, at about 4×10^{-8} ohm m^2, was double that observed on the lead electrode, presumably due to the presence of the dielectic PTFE phase in the bonded catalyst. This value compares with 5×10^{-9} and 5×10^{-8} ohm m^2 for *ex situ* resistance measurements on 10^{-5} m thick PTFE-bonded PbO_2 films on glass.

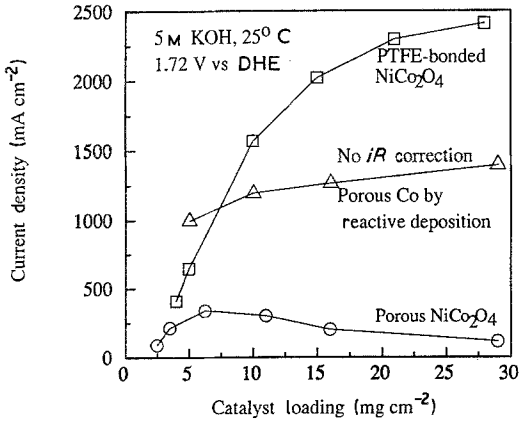

Fig. 10. Effect of catalyst loading on anode performance for O_2 evolution in 5 kmol m^{-3} KOH at 298 K, 1.720 V vs DHE.

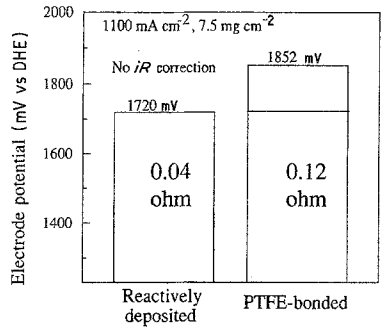

Fig. 11. Comparison of the effect of ohmic potential losses on reactively deposited Co and PTFE-bonded $NiCo_2O_4$.

4. Reactively deposited Co electrodes

A novel method, reactive deposition, has been invented by Tseung *et al.* [12]. The porous Co electrodes produced by reactive deposition had a controlled structure to maximize the electrochemically active area. Scanning electron microscopy showed that it was composed of $\sim 0.1\ \mu$m fine pore and $\sim 1\ \mu$m coarse pore structures, intimately interwoven, with similarly sized metal grains. These grains were joined together metallurgically, resulting in a higher conductivity compared with PTFE-bonded electrodes. Figure 10 shows the performance of such an electrode compared with some published results [13] on PTFE-bonded and non-PTFE-bonded porous $NiCo_2O_4$ electrodes.

It is important to note that the results for the reactively deposited Co electrode, unlike the other two electrodes, have not been corrected for *iR* potential losses. When these are taken into account (Fig. 11), the performance at 1 A cm^{-2} is better than the PTFE-bonded electrode. It is possible that during the initial stages of oxygen evolution, the electrolytes in the coarse pores are expelled first, leaving open channels for the gas from the fine pores to escape, analogous to the operation of PTFE-bonded electrodes. This ensures better utilization of available cobalt area. This, coupled with the absence of the inert and non-conducting PTFE particles and their higher conductivity, accounts for their better performance. Attempts to reactively deposit acid-resistant porous electrodes are in progress.

5. Conclusions

The results to date have shown that it is possible to decrease the oxygen evolution overpotential with PTFE/β-PbO_2 catalysts on Pb, but the sintering conditions need to be carefully controlled to avoid significant PbO_2 thermal reduction and oxygen loss. However, oxidation of the Pb substrate causing catalyst shedding is an outstanding problem. The resistance of the PTFE-bonded catalyst layer measured *in situ* using a 10 kHz a.c. potential perturbation, was not significantly greater than on electrochemical oxidized Pb alone and is not responsible for the less than expected improvement in performance on adding the PTFE-bonded PbO_2 catalyst layer.

Reactive depositions of Co has been shown to offer a potentially simple route to porous anodes for gas evolution, at least in alkaline electrolytes. Work is in progress to produce porous metals with acid-stable oxides.

Acknowledgements

The authors thank the EEC and the Mineral Industry Research Organisation (MIRO) for financial support of the project.

References

[1] V. A. Ettel and B. V. Tilak, in 'Comprehensive Treatise on Electrochemistry' (edited by J. O.'M. Bockris, B. E. Conway, E. Yaeger and R. E. White), Plenum, New York (1981) Vol. 2, Ch. 6, pp. 327–380.

[2] A. J. Monhemius, in 'Topics in Non-Ferrous Extractive Metallurgy' (edited by A. R. Burkin), Blackwell Scientific, Oxford (1980).

[3] A. D. S. Tantram and A. C. C. Tseung, *Nature* **221** (1969) 167.

[4] P. Jones, R. Lind and W. F. K. Wynne-Jones, *Trans. Faraday Soc.* **50** (1958) 972.

[5] W. Mindt, *J. Electrochem. Soc.* **116** (1969) 1076.

[6] L. J. van der Pauw, *Phillips Res. Rep.* **13** (1958) 1.

[7] R. E. Meredith and C. W. Tobias, in 'Advances in Electrochemistry and Electrochemical Engineering' (edited by C. W. Tobias and P. Delahay), Academic, New York (1966).

[8] D. A. G. Bruggeman, *Ann. Physik.* **636** (1935) 24.

[9] A. J. Bard, J. Jordan and R. Parsons (eds), 'Standard Potentials in Aqueous Solutions', Decker, New York (1985).

[10] I. Barin and O. Knacke, 'Thermochemical Properties of Inorganic Substances', Springer, Berlin (1973).

[11] R. L. Deutscher, S. Fletcher and J. A. Hamilton, *Electrochim. Acta.* **31** (1986) 585.

[12] A. C. C. Tseung, S. P. Jiang, Y. K. Chen and J. K. You, UK Patent Application, 88.154943, 29 June (1988).

[13] A. C. C. Tseung, *J. Appl. Electrochem.* **15** (1985) 575.